JOURNAL OF THEORETICAL
AND APPLIED MECHANICS
51, 2, pp. 431-438, Warsaw 2013

THE UNSTEADINESS OF TIP CLEARANCE FLOW AND ITS EFFECT TO STABILITY OF TRANSONIC AXIAL COMPRESSOR

J.F. Hu, X.C. ZHu, H. Ou-Yang, J. Tian, Y.D. Wu, X.Q. Qiang, G. ZHao, Z.H. Du
Shanghai JiaoTong University, School of Mechanical Engineering, Shanghai, China
e-mail: huli2003@163.com

The steady and unsteady RANS simulations of a transonic compressor rotor (NASA rotor 37) are performed to investigate the tip clearance flow characteristic and correlations between tip leakage flow and compressor stability. For steady simulations, the results are compared with the aerodynamic probe and laser anemometer data. The speed lines and span-wise aerodynamic parameters agree well with the experimental data. On the other hand, the tip clearance flow of unsteady simulations are analysed clearly at a near stall condition. The results show that there is a mass flow rate boundary. The tip clearance flow oscillates substantially with a frequency about 50% BPF when the mass is less than that, which is caused by tip clearance flow, shock, and the interaction between them and the oncoming flow. The interface between the oncoming flow and clearance flow shifts forward, and the tip clearance flow may spill over into the adjacent blade passage as the mass flow decreases, which may results in the spike stall inception.

Key words: tip leakage flow, compressor, stability

1. Introduction

The axial flow compressor is one of the most important parts in modern gas turbines. It is critical to maintain a suitable stall margin with increased aerodynamic blade loading of it. Many researchers have reported some methods in order to increase the stall margin. However, it is important to understand the detailed flow structures in blade rows near stall firstly, which may induce rotating stall. As we all kown, tip clearance flows plays dominant and important parts in axial compressor aerodynamics because it has a great influence on the stability.

Tip clearance flows were studied experimentally and computationally to investigate the relations of stall inception in the from last century (Adamczyk *et al.*, 1993; Copenhaver *et al.*, 1996; Hoying *et al.*, 1999; Hah and Loellbach, 1999; Yamada *et al.*, 2003; Hah *et al.*, 2006). Recently, Hah *et al.* (2008) conducted unsteady three-dimensional numerical simulation for a transonic axial compressor rotor and noted that the tip clearance vortex originates near the leading edge. The low momentum area builds up immediately downstream of the passage shock and prevents the incoming flow from passing through the pressure side of the passage and initiates stall inception. Vo *et al.* (2005) developed criteria for spike stall inception. Hah *et al.* (2010) found one frequency of 80Hz except that of the oscillating tip clearance vortex. The larger blockage area spanned several consecutive blade passages, and flow near the leading edge spilled over into the adjacent blade passage.

The purpose of the current study is to clarify the tip flow field in a transonic axial compressor rotor at a near stall condition, and to investigate correlations between the tip clearance flow and compressor stability. The unsteady behavior of tip flow fields in the transonic compressor rotor at the two conditions have been investigated by unsteady three-dimensional Navier-Stokes flow simulations. With the comparison between FFT analysis of the two conditions, there is a critical mass flow rate point, which is the boundary of tip clearance flow oscillation. As the mass flow

rate decreases, the intersection surface caused by the oncoming flow and the tip clearance flow shifts forward, and that may induce short length stall inception when the mass flow rate continue desreasing to a certain extent.

2. Numerical model and method

2.1. Numerical model

NASA Rotor 37 is researched in the present work, which is a transonic axial compressor rotor, originally designed and tested at NASA Lewis Research Center in the 1970's. The rotor has 36 blades with an aspect ratio of 1.19 and a hub-tip ratio of 0.7. The inlet Mach number is 1.48 at the tip at the design speed of 17188.7 rpm. The design mass flow is 20.19 kg/s and pressure ratio is 2.106. The choke mass flow is about 20.93 kg/s. The running tip clearance was estimated to be 0.0356 cm for the blind test case using both touch probe and rub probe measurements.

2.2. Numerical method

The steady and unsteady simulations are carried out to investigate the tip clearance flow by solving unsteady three-dimensional, Reynolds-averaged Navier-Stokes equations, through commercial solver package, CFX. This solver is based on the finite volume scheme and utilizes second-order high precision discretization scheme. The κ-ε turbulence model and standard wall function are used to account for the turbulence flow. The 20 physical time steps per blade passage and 10 inner iterations are performed at each time step for time accurate simulation in the present work.

The grid is constructed by CFX-Turbogrid shown in Fig. 1a. The computational domain was divided into two parts with a composite grid system in present simulation. One part is the main flow region outside the blade tip clearance, and the other is the tip clearance region. Figure 1b shows the monitor distributions at the tip area.

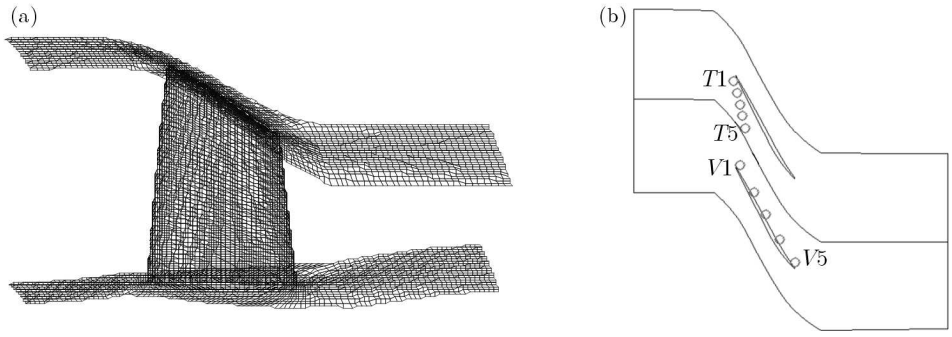

Fig. 1. (a) The computational model grids; (b) the monitor distributions at the tip area

3. Results and discussion

3.1. Validity of numerical simulation

The comparison of the computed and experimental total pressure ratio characteristic is depicted in Fig. 2. The simulations for this compressor rotor are all conducted at the design rotational speed with various back pressures. All mass flow rates were corrected by the value at choke. In Fig. 3, it is seen that the predictions are somewhat less than the experimental data. The trend of the total pressure ratio agree very well with the experimental results. The

predicted mass flow ratio at the near stall condition is slightly less than the experimental data. The unsteady simulations of conditions I-NS are here conducted based on the steady simulation.

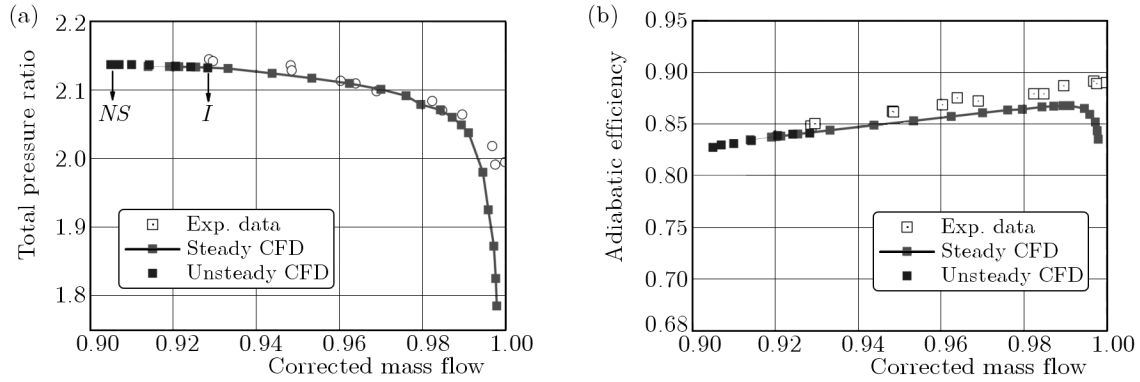

Fig. 2. Characteristic curves of the compressor rotor

In order to demonstrate validity of the numerical simulations and grids in the blade row, some pitchwise mass averaged comparisons along the blade span are made at two conditions, near the peak efficiency and near stall conditions. Figure 3 shows the span-wise distribution of the total pressure ratio and adiabatic efficiency at the near peak efficiency condition. The trend of pressure ratio is very close to the experiment except that around hub. The computed efficiency is lower than the experimental one except the tip, but the tendency follows the experimental data generally. Figure 4 shows the span-wise distributions of the total pressure ratio and adiabatic

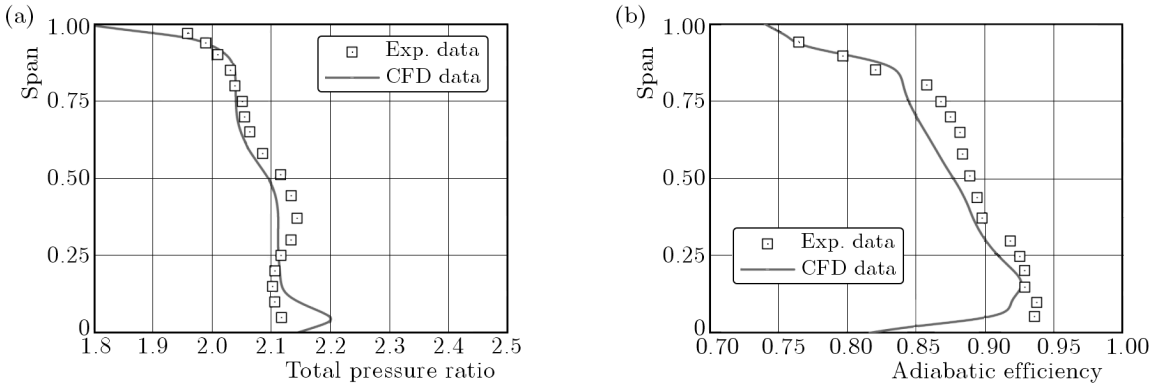

Fig. 3. The span-wise distributions of total pressure ratio and adiabatic efficiency at near peark efficiency condition

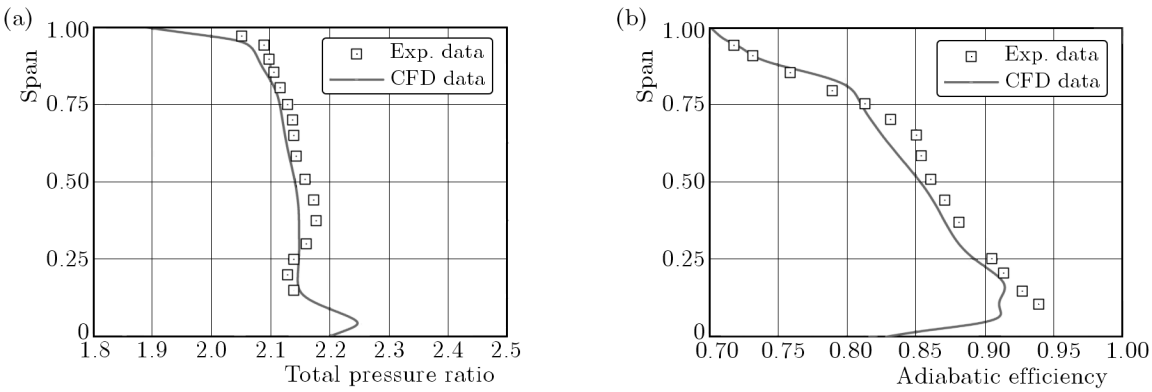

Fig. 4. The span-wise distributions of total pressure ratio and adiabatic efficiency at near stall condition

efficiency near stall. The trends of them are all similar to the ones at NPE condition. The largest error area is also in the hub region. However, the simulation result has a good agreement with the experimental data near the tip region. It is considered quite good for analyzing the tip clearance flow field in the rotor.

Figures 5 show comparison of the experimental and computational relative Mach number contour at 95% span at the near stall condition. The numerical result agrees well with the experimental data. The interaction of tip clearance flow and shock is very intense, and that induces the breakdown of the tip leakage vortex. A large area of low momentum appears downstream of the passage shock, and leading to a large blockage and unsteadiness in the rotor tip.

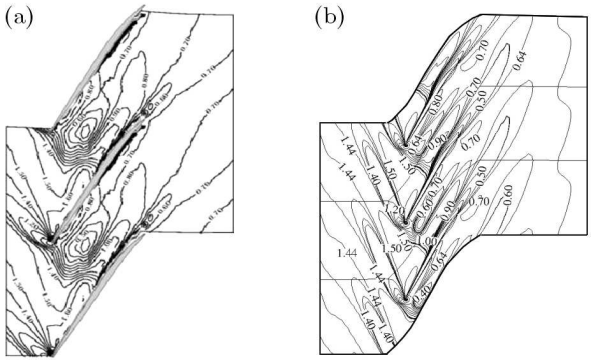

Fig. 5. The contour of blade-to-blade Mach number, 95% span, near stall, experimental (a), and numerical Mach number contours (b)

3.2. Unsteady tip clearance flow characteristics

In order to investigate the unsteadiness of the tip clearance at the near stall condition, two conditions are calculated based on the steady simulations, which can be seen in Fig. 2. Ten numerical monitors are located with various axial positions on the tip area for unsteady static pressure values. The results of a Fast Fourier Transformation (FFT) process of monitors are given in Fig. 6 at operating condition I. It can be seen that the frequency the same as the blade passing frequency (BPF). This phenomenon indicates that there are no oscillations in the tip clearance flow at this operating condition. But with the FFT analysis of unsteady static pressure at the near stall condition, it can be found that a dominant frequency of about 50% of the blade passing frequency is observed at all monitors. This is the tip clearance flow oscillation frequency, which indicates that the unsteadiness of the tip flow is intensified as the mass flow decreases. Because the oscillation does not appear at condition I, it means that there is a boundary between two these conditions as the oscillation dividing point.

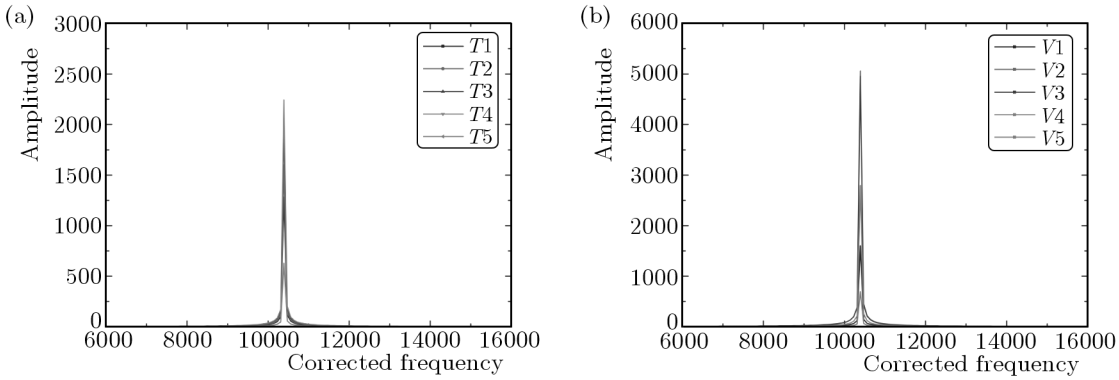

Fig. 6. Unsteady static pressure frequency and amplitude of monitors at condition I

Figure 7 shows relative RMS values of suction and pressure surface static pressure from the unsteady simulation at the near stall condition. From the figures, we can see that the intensity of tip clearance oscillation becomes larger at the biger radius of the blade, and the oscillation intensity of the pressure surface is larger than the suction one. Figure 8 shows relative RMS values of static pressure at 30%, 80%, 98.5% span. The intensity near pressure surface leading edge, shock wave and tip clearance vortex is larger than any other areas. Above all, it implies that unsteadiness at the tip have main relations with the tip clearance vortex, shock and oncoming flow.

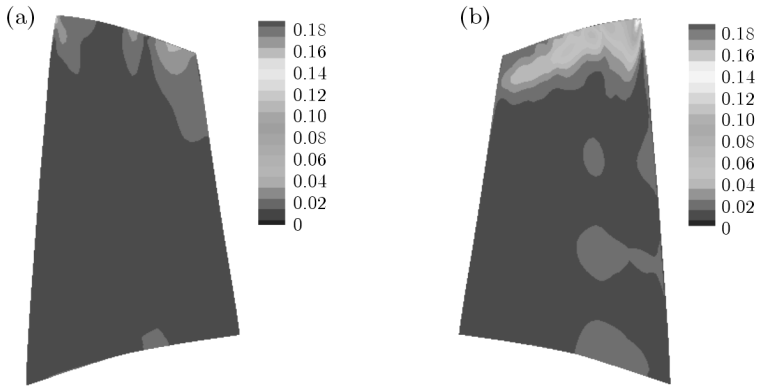

Fig. 7. Sstatic pressure RMS distributions at suction and pressure surfaces, suction (a), and pressure (b)

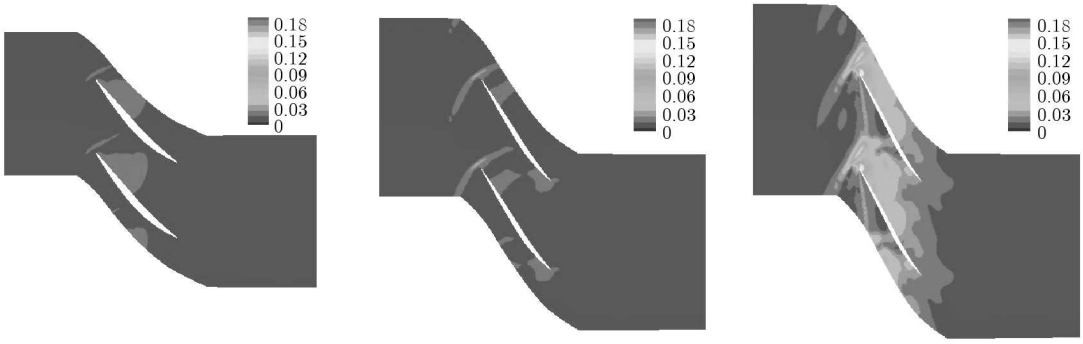

Fig. 8. Static pressure RMS distributions at 30%, 80%, 98.5% span

3.3. Effect of tip clearance flow to stability of axial compressor

According to the results at condition I and near stall, we find two different kinds of the unsteadiness. One is the inherent unsteadiness. Another is the tip clearance flow oscilation unsteadiness. This indicates that the tip clearance flow oscillates as the mass flow decreases to one critical condition. Recently, in the stall inception research field of the axial compressor, Vo *et al.* (2005) pointed out two necessary conditions for short-length stall inception. One is that the interface between the tip clearance and oncoming flows become parallel to the leading-edge plane. The second is the initiation of backflow at the trailing-edge plane. Hah *et al.* (2006) validated this theory to be also suitable for transonic axial compressor. The effect of the tip clearance flow on stability of the axial compressor is analysed here according to Vo's theory.

From many research reports, the distribution of relative total pressure or entropy can indicate the loss and interface between the incoming and tip clearance flows. Figures 9 and 10 depict the time average entropy and velocity vector at 98.5% span at conditions I and near stall. From the figures, we can see that the interface at the near stall condition is closer to the leading edge than

condition I. The intensity of the tip clearance vortex and shock wave become larger as the mass flow decreases. The tip clearance vortex breaks down, and larger low momentum area appears, which leads to the large blockage effect near the tip. Above phenomenona make the interface shifts forward. At the same time, the oncoming flow may turn its direction, and enlarge the inflow angle at the leading edge to a certain extent, which can produce a detached flow there and compressor instability.

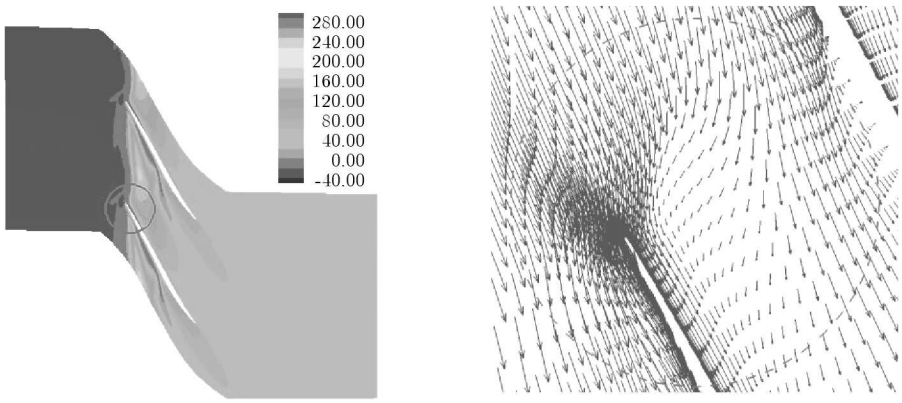

Fig. 9. Time average entropy and velocity vector at 98.5% span at condition I

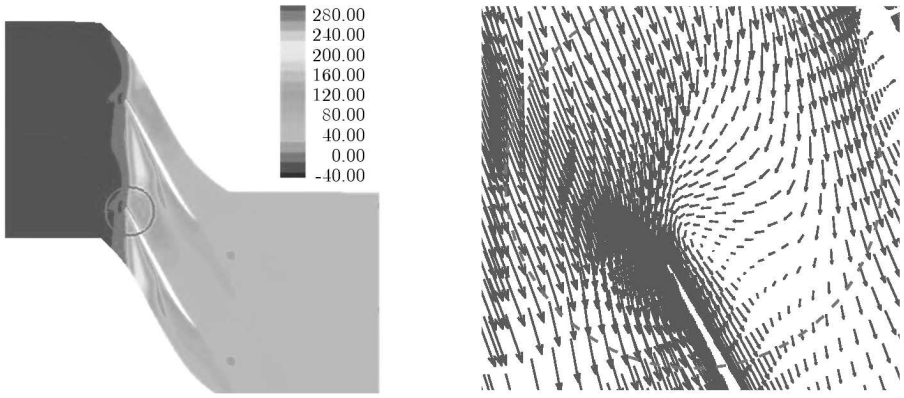

Fig. 10. Time average entropy and velocity vector at 98.5% span at near stall condition

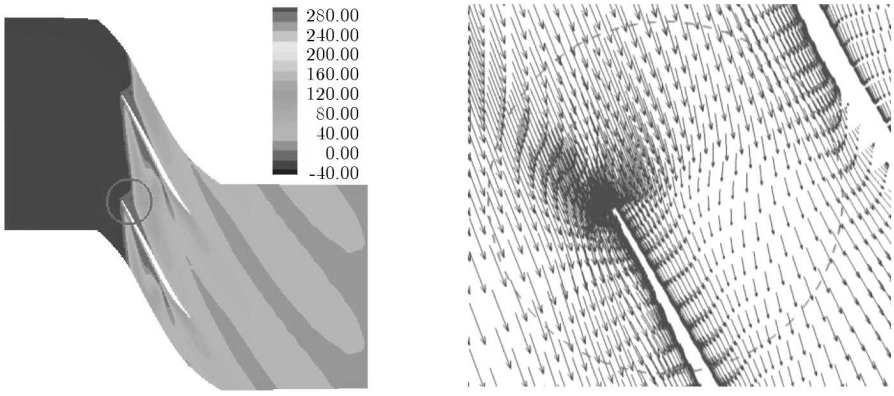

Fig. 11. Entropy and velocity vector at 98.5% span at near peak efficiency condition

Figure 11 shows the entropy and velocity vector at 98.5% span at the near peak efficiency condition. It can be clearly seen that the interface deviates more from the leading edge than

condition I and near stall. Because of lower intensity of the tip clearance flow and shock, the interface shifts downstream to sustain the surface as the result of balance between the tip clearance flow and the oncoming flows. Figure 12 displays the interface locations at four conditions, condition I, near stall, near peak efficiency and one transition condition between them. X and Y are the computational area coordinates. The interface shifts more forward generally when the mass flow decreases more. The positions deviate little near the suction surface, and larger in the approaching process to pressure surface at four conditions. The interface may shift forward when the mass flow decreases more, thus the tip cleareace flow could spill over into the adjacent blade passage, and cause compressor instability.

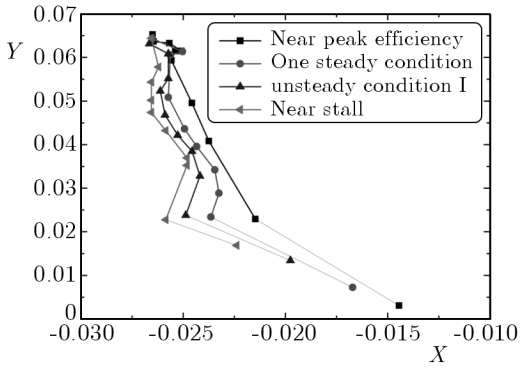

Fig. 12. Location of intersection surfaces for four conditions

4. Conclusion

The tip clearance flow fields in the transonic axial compressor rotor have been investigated by steady and unsteady RANS simulations. Through the contrast of the tip clearance flow characteristic at condition I, near efficiency, near stall and one steady condition, the results can be summarized as follows:

- With the FFT analysis of unsteady static pressure, the tip clearance flow oscillates at about 50% BPF for the unsteady near stall condition in contrast to condition I. This phenomenon indicates that there is a critical mass flow point which is the transition point for oscillation. The oscillation intensity of the pressure surface is larger than the suction one. The largest intensity appears near the pressure surface leading edge. With a higher height of the blade, the tip clearance oscillation has larger intensity.
- As the mass flow decreases, the intensity of the tip clearance vortex, shock and interaction between them strengthens, which makes induces the interface between the incoming flow and tip clearance flow shift forward after the balance of them. At the same time, the inlet flow angle at the adjacent blade passage increases, and generates a detached flow at the leading edge. As the mass flow decreases to a certain extent, the interface becomes parallel with the leading edge, and the tip clearance flow may spill into the adjacent blade passage. Therefore, that may result in spike-type rotating stall inception.

Acknowledgment

This work was supported by National Natural Science Foundation of China, Grant 51076101, 11202132 and Shanghai Municipal Education Commission Innovation Foundation 11CXY07. The author would like to acknowledge these supports.

References

1. Adamczyk J.J., Celestina M.L., Greitzer E.M., 1993, The role of tip clearance in high-speed fan stall, *ASME Journal of Turbomachinery*, **115**, 28-38
2. Copenhaver W.W., Mayhew E.R., Hah C., Wadia A.R., 1996, The effects of tip clearance on a swept transonic compressor rotor, *ASME Journal of Turbomachinery*, **118**, 230-239
3. Hah C., Bergner J., Schiffer H.P., 2006, Short length-scale rotating stall inception in a transonic axial compressor-criteria and mechanisms, *ASME Paper*, **2006-GT-90045**
4. Hah C., Bergner J., Schiffer H.P., 2008, Tip clearance vortex oscillation, vortex shedding and rotating instabilities in an axial transonic compressor rotor, *ASME Paper*, **GT2008-50105**
5. Hah C., Voges M., Muller M., Schiffer H.P., 2010, Characteristics of tip Clearence flow instability in a transonic compressor, *ASME Paper*, **GT2010-22101**
6. Hah C., Loellbach J., 1999, Development of hub corner stall and its influence on the performance of axial compressor blade rows, *ASME Journal of Turbomachinery*, **121**, 1, 67-77
7. Hoying D.A., Tan C.S., Vo H.D., Greitzer E.M., 1999, Role of blade passage flow structures in axial compressor rotating stall inception, *ASME Journal of Turbomachinery*, **121**, 735-742
8. Vo H.D., Tan C.S., Greitzer E.M., 2005, Criteria for spike initiated rotating stall, *ASME Paper*, **GT2005-68374**
9. Yamada K., Furukawa M., Inoue M., Funazaki K., 2003, Numerical Analysis of Tip Leakage Flow Field in a Transonic Axial Compressor Rotor, *International Gas Turbine Congress Proceedings, IGTC Paper 2003*, 095

Nieustaloność przepływu w szczelinie wierzchołkowej i jej wpływ na stabilność pracy przydźwiękowej sprężarki osiowej

Streszczenie

W pracy przedstawiono symulacje stanu ustalonego i nieustalonego przydźwiękowej sprężarki osiowej (turbina NASA 37) z zastosowaniem metody Reynoldsa uśredniania równań Naviera-Stokesa (RANS) w celu zbadania charakterystyki przepływu w szczelinie wierzchołkowej oraz określenia zależności pomiędzy stratami związanymi z upływem w tej szczelinie a stabilnością pracy sprężarki. Wyniki symulacji stanu ustalonego porównano z danymi doświadczalnymi uzyskanymi za pomocą sondy aerodynamicznej i laserowego wiatromierza. Wyznaczone wzdłuż rozpiętości sprężarki linie prędkości przepływu i jego parametry aerodynamiczne okazały się zgodne z danymi doświadczalnymi. W przypadku symulacji stanu nieustalonego, analizę przepływu w szczelinie wierzchołkowej przeprowadzono dla warunków bliskich oderwania, tj. utraty wydajności sprężarki, wyznaczając graniczny wydatek przepływu dla takiej sytuacji. Poniżej tej granicznej wartości, zmiany przepływu w szczelinie oscylują z częstotliwością sięgającą 50% częstotliwości przejścia łopatek (tzw. BPF), co jest konsekwencją interakcji wywołanej zderzeniem przepływu z falą napływową w szczelinie wierzchołkowej. Powierzchnia tej interakcji przesuwa się do przodu, a sam przepływ może rozpaść się na fragmenty znajdujące ujście w kanałach przyległych łopatek. Zjawisko to zachodzi przy malejącym wydatku, a to z kolei może indukować oderwanie przepływu skokowymi zmianami mocy współpracującego silnika.

Manuscript received January 11, 2012; accepted for print September 4, 2012